**Repurposing low-molecular-weight drugs against the main protease of SARS-CoV-2**

Jia Gao[#], Liang Zhang[#], Xiaodan Liu, Fudong Li, Rongsheng Ma, Zhongliang Zhu, Jiahai Zhang, Jihui Wu, Yunyu Shi, Yueyin Pan, Yushu Ge[*], Ke Ruan[*]

[1]Ministry of Education Key Laboratory for Membrane-less Organelles & Cellular Dynamics, Hefei National Laboratory for Physical Sciences at the Microscale, Division of Life Sciences and Medicine, University of Science and Technology of China, 230027, Hefei, P. R. China

[#] J.G. and L.Z. contributed equally to this work.

[*]To whom correspondence may be addressed. Email: kruan@ustc.edu.cn (K.R.), geyushu@ustc.edu.cn (Y.G.)

**Abstract**

The pandemic of COVID-19, which is caused by the SARS-CoV-2 virus infection, has posed a threat to global healthcare system. The repurposing drug is one of the feasible ways for the emergency treatment. As the low-molecular-weight drugs have a higher possibility to fully match the interactions with essential targets of SARS-CoV-2, we propose a strategy to uncover such drugs using the fragment-based approach.Here, using the ligand-observed and protein-observed fragment screening approach, we identified niacin and hit **1** binding to the catalytic pocket of the main protease of SARS-CoV-2 ($M^{pro}$), thus modestlyinhibited the enzymatic activity of $M^{pro}$.The chemical shift perturbations induced by niacin and hit **1** indicates a partial overlap of their binding sites, i.e., the catalytic pocket of $M^{pro}$ may accommodate derivatives with larger molecular size. We hence searched drugs containing the niacin or hit **1** pharmocophore,and uncovered carmofur, bendamustine, triclabendazole and emedastine, which demonstrated higher potency of inhibiting protease activity than the fragment screening hits. Our work demonstrated that fragment-based approach is a feasible way to uncover low-molecular-weight drugs against SARS-CoV-2, and potentially other targets without specific drug yet.

**Keywords:** novel coronavirus, SARS-CoV-2, main protease, fragment-based screening

The outbreak of COVID-19 caused by SARS-CoV-2 virus infection[1-3] has so far affected over 3 million people worldwide, at a mortality rate of around 7%. One of the most extensively studied targets of coronaviruses is the main protease ($M^{pro}$or $3CL^{pro}$)[4].$M^{pro}$ plays an essential role in cleavage of the virus polypeptide translated from the viral RNA[5], and $M^{pro}$ recognizes at least 11 cleavage site in the virus protein 1ab, e.g., LQ↓SAG (↓denotes the cleavage site). The covalent inhibitors against the SARS-CoV-2 $M^{pro}$ have recently demonstrated potency in the inhibition of viral replication in cellular assays[6,7], which further underpins the druggability of $M^{pro}$. However, these compounds are at the early stage of preclinical studies, and the development of a new drug usually takes years. The lack of drugs targeting SARS-CoV-2currently poses a lifethreat to numerous COVID-19 patients.

The pandemic of COVID-19 urges the discovery of a repurposing oral drug[8].Since most drugs recently approved were designed and optimized for specific targets, such complex compounds were unlikely to fully match the interactions with the targets of SARS-CoV-2. The fact is that the estimated number of drug-like compounds (molecular weight of 500 Da approximately) is ca. $10^{60}$, in comparison with 13550 potential drugs in Drugbank at various stages from preclinical studies to approval. Therefore, the possibility to uncover a highly potent and specific drug against SARS-CoV-2 is quite slim.Conversely, low-molecular-weight drugswith intermediate potency and high safety can be an alternative way against SARS-CoV-2. The toxicity of many low-molecular-weight drugs were well understood as they were often in clinics for years. Furthermore, their relative lower structural complexity adds odds to fully match the interactions with anti-SARS-CoV-2 targets, e.g., the chemical space of compounds with less than 11 non-hydrogen atoms is ca. $10^{9}$.This is the cornerstoneof fragment-based lead discovery[9], and

many of the compounds in fragment library were indeed extracted from pharmocophores of the approved drugs. We hence hypothesize that it is of high probability to uncover a low-molecular-weight drug containing pharmacophores identified by fragment-based screening (FBS).

We hence assessed 38 compounds in our fragment library, which are the pharmacophores(substructures) of the repurposing drugs proposed from virtual screening[10-15] against the SARS-CoV-2 target.Since these candidates are predicted to bind at a high affinity, their pharmacophores should bind as well, although at a weaker affinity.These weak binders can be readily identified using NMR fragment-based approach, thus eliminate the distracting false positives in virtual screening.Using our NMR fragment-based approach[16-18], we characterized the weak target-ligand interactions using ligand-observed spectra, e.g., saturation transfer difference (STD) and WaterLOGSY. Three hits of SARS-CoV-2 $M^{pro}$were henceidentified (Figure 1a), i.e., niacin, hit **1** and **2** (Figure 1b).Potency of these three hit were then evaluated using the enzymatic activity assay of SARS-CoV-2 $M^{pro}$(Figure 1c). Niacin and hit **1**moderately inhibited the cleavage of fluorescence labeled polypeptide (FITC-AVLQSGFR-Lys(Dnp)-Lys-NH2) by SARS-CoV-2 $M^{pro}$.

To further map the binding sites of niacin and hit **1**, we determined chemical shift perturbations (CSPs)of $^{15}$N-labeled $M^{pro}$induced by the titration of these two compounds. Due to the severe signal overlap in the fingerprint HSQC (heteronuclear single-quantum correlation) spectrum of the $^{15}$N labeled full-length SARS-CoV-2 $M^{pro}$ (residue 4-306),the N-terminal domain($M^{pro}$-N) with the catalytic core included(residue 4-199) was used instead for all protein-observed NMR studiesthereafter. The well-dispersed HSQC spectrum of SARS-CoV-2 $M^{pro}$-N enabled many $^{1}$H-$^{15}$N amide chemical shift assignments transferred directly from

SARS-CoV $M^{pro}$-N[19], as these two protein shares 96% sequence identity. Key residues proximal to the catalytic site were thus assigned, including H41, V42, D48, N51,G143, H163, V186, etc.(Figure S1). Both niacin and hit **1** perturbs a common residue V42, suggesting these two hits bind to the catalytic core of SARS-CoV-2 $M^{pro}$. Interestingly, these two hits also recognize different sets of residues in the catalytic core, e.g., niacin perturbs H41, G143, N51, V186 (Figure 2a), while hit **1** induces CSPs of residues M165,E166, L167 (Figure 2b). Mapping these residues to the surface representation of the crystal structure of SARS-CoV-2 $M^{pro}$(PDB code: 6LU7)[6]suggests that these two hits adopt different orientations in the catalytic site with a shared anchor point near V42 (Figure 2c). Taken into account of the molecular size of niacin and the spatial distribution of the perturbed residues, niacin probably binds to more than one site. Nevertheless,the CSP pattern suggests that the catalytic core of SARS-CoV-2 $M^{pro}$may accommodate compounds of larger size than niacin and hit **1**.

We hence searched low-molecular-weight (less than 400 Da) drugs containing the pharmacophores of niacin and hit **1**. Molecular docking nominates carmofur as a niacin derivative. Titration of carmofur to $^{15}$N-labeled SARS-CoV-2 $M^{pro}$-N induced an extra setof cross peaks at a ligand/protein molar ratio of 2:1, and some original signals completely disappeared at the molar ratio of 4:1 (Figure S2a). This is an indication of a strong binding between carmofur and SARS-CoV-2 $M^{pro}$, as confirmed by the $IC_{50}$ of 2.8 ± 0.2 μM determined by the enzymatic assay at the $M^{pro}$ concentration of 0.5 μM(Figure S2b).However, the complete disappearance of original NMR signals occurs at a ligand/protein molar ratio significantly deviated from a stoichiometry of 1:1. It has been recently demonstrated that carmofur is a covalent inhibitor of the main protease of SARS-CoV-2 with a $IC_{50}$value of 1.82 μM in the presence of 0.2 μM enzyme[6], consistent with

our measurement as a higher $M^{pro}$ concentration was used in our case. Collectively, these data suggest that the covalent linking to SARS-CoV-2 $M^{pro}$ is driven by excess carmofur. Nevertheless, it is a feasible way to repurpose low-molecular-weight drugs targeting SARS-CoV-2 $M^{pro}$ using this fragment-based approach.

Further pharmacophore searching and molecular docking nominates several low-molecular-weight analogs of hit **1**, e.g., triclabendazole, emedastine andbendamustine (Figure S3a).The single-dose enzymatic assay shows these three drugs have significantly higher potency than hit **1** (Figure S3b)**.** We further determine the dose dependent response of bendamustine and emedastine in the inhibition of SARS-CoV-2 $M^{pro}$ activity, with $IC_{50}$values of 26 ± 1 μM and 82 ± 7 μM(Figure 3a).The $IC_{50}$ value of triclabendazole was roughly estimated as 70 μM from the two-dose inhibition rates (31% and 72% inhibition at 50μM and100 μM triclabendazole, respectively), as limited by the low aqueous solubility of tricalbendazole.Bendamustine and emedastine also induced significantly larger CSPs in a dose-dependent manner than hit **1**(Figure 3b).

Taken together, our fragment-based strategy facilitates the discovery of low-molecular-weight drugs against SARS-CoV-2 $M^{pro}$. First, this approachcan be readily applied to identify low-molecular-weight drugs against other SARS-CoV-2 targets, e.g., RNA-dependent RNA polymerase or the receptor binding domain of the spike protein.Second, a cocktail of these low-molecular-weight drugs could be considered to gain a higher potency than a single compound, if their binding topologies show no evidence of steric repulsion.Finally, although carmofur and bendamustine show higher potency than the fragment screening hits, the toxicity of anti-cancer drugs remains a challenge in its clinical applications. Conversely, triclabendazole

and emedastine could be valuable in the inhibition of SARS-CoV-2 virus replication at the early-stage. It could also serve as a starting point of the next round of pharmacorphore searching. In general, our study shall pave a new way towards the repurposing of low-molecular-weight drugs against SARS-CoV-2, and other potential targets without specific drugs developed yet.

**ACKNOWLEDGMENT**

Part of our NMR work was performed at the National Center for Protein Science Shanghai andthe High Magnetic Field Laboratory of the Chinese Academy of Sciences. We thank the financial support from the Ministry of Science and Technology of China (Grant No. 2016YFA0500700 and 2014CB910604), the National Natural Science Foundation of China (Grant No. 21874123, 21703254 and 21807095), the Fundamental Research Funds for the Central Universities (WK2060190086), andsupercomputing resources from the Bioinformatics Center of the University of Science and Technology of China, School of Life Sciences.

**REFERENCES**

(1) Chen, N.; Zhou, M.; Dong, X.; Qu, J.; Gong, F.; Han, Y.; Qiu, Y.; Wang, J.; Liu, Y.; Wei, Y.; Xia, J. a.; Yu, T.; Zhang, X.; Zhang, L. Epidemiological and clinical characteristics of 99 cases of 2019 novel coronavirus pneumonia in Wuhan, China: a descriptive study. *Lancet***2020**, *395*, 507-513.

(2) Li, Q.; Guan, X.; Wu, P.; Wang, X.; Zhou, L.; Tong, Y.; Ren, R.; Leung, K. S. M.; Lau, E. H. Y.; Wong, J. Y.; Xing, X.; Xiang, N.; Wu, Y.; Li, C.; Chen, Q.; Li, D.; Liu, T.; Zhao, J.; Liu, M.; Tu, W.; Chen, C.; Jin, L.; Yang, R.; Wang, Q.; Zhou, S.; Wang, R.; Liu, H.; Luo, Y.; Liu, Y.; Shao, G.; Li, H.; Tao, Z.; Yang, Y.; Deng, Z.; Liu, B.; Ma, Z.; Zhang, Y.; Shi, G.; Lam, T. T. Y.; Wu, J. T.; Gao, G. F.; Cowling, B. J.; Yang, B.; Leung, G. M.; Feng, Z. Early Transmission Dynamics in Wuhan, China, of Novel Coronavirus-Infected Pneumonia. *The New England journal of medicine***2020**, *382*, 1199-1207.

(3) Wu, F.; Zhao, S.; Yu, B.; Chen, Y.-M.; Wang, W.; Song, Z.-G.; Hu, Y.; Tao, Z.-W.; Tian, J.-H.; Pei, Y.-Y.; Yuan, M.-L.; Zhang, Y.-L.; Dai, F.-H.; Liu, Y.; Wang, Q.-M.; Zheng, J.-J.; Xu, L.; Holmes, E. C.; Zhang, Y.-Z. A new coronavirus associated with human respiratory disease in China (vol 579, pg 265, 2020). *Nature***2020**.

(4) Anand, K.; Ziebuhr, J.; Wadhwani, P.; Mesters, J. R.; Hilgenfeld, R. Coronavirus main

proteinase (3CL(pro)) structure: Basis for design of anti-SARS drugs. *Science***2003**, *300*, 1763-1767.

(5) Hilgenfeld, R. From SARS to MERS: crystallographic studies on coronaviral proteases enable antiviral drug design. *Febs Journal***2014**, *281*, 4085-4096.

(6) Jin, Z.; Du, X.; Xu, Y.; Deng, Y.; Liu, M.; Zhao, Y.; Zhang, B.; Li, X.; Zhang, L.; Peng, C.; Duan, Y.; Yu, J.; Wang, L.; Yang, K.; Liu, F.; Jiang, R.; Yang, X.; You, T.; Liu, X.; Yang, X.; Bai, F.; Liu, H.; Liu, X.; Guddat, L. W.; Xu, W.; Xiao, G.; Qin, C.; Shi, Z.; Jiang, H.; Rao, Z.; Yang, H. Structure of Mpro from COVID-19 virus and discovery of its inhibitors. *Nature***2020**.

(7) Zhang, L.; Lin, D.; Sun, X.; Curth, U.; Drosten, C.; Sauerhering, L.; Becker, S.; Rox, K.; Hilgenfeld, R. Crystal structure of SARS-CoV-2 main protease provides a basis for design of improved alpha-ketoamide inhibitors. *Science (New York, N.Y.)***2020**.

(8) Li, G.; De Clercq, E. Therapeutic options for the 2019 novel coronavirus (2019-nCoV). *Nature Reviews Drug Discovery***2020**, *19*, 149-150.

(9) Murray, C. W.; Rees, D. C. The rise of fragment-based drug discovery. *Nature Chemistry***2009**, *1*, 187-192.

(10) Chen, Y. W.; Yiu, C.-P. B.; Wong, K.-Y. Prediction of the SARS-CoV-2 (2019-nCoV) 3C-like protease (3CL pro) structure: virtual screening reveals velpatasvir, ledipasvir, and other drug repurposing candidates. *F1000Research***2020**, *9*, 129-129.

(11) Kandeel, M.; Al-Nazawi, M. Virtual screening and repurposing of FDA approved drugs against COVID-19 main protease. *Life sciences***2020**, *251*, 117627-117627.

(12) Liu, S.; Zheng, Q.; Wang, Z. Potential covalent drugs targeting the main protease of the SARS-CoV-2 coronavirus. *Bioinformatics (Oxford, England)***2020**.

(13) Ortega, J. T.; Serrano, M. L.; Pujol, F. H.; Rangel, H. R. Unrevealing sequence and structural features of novel coronavirus using in silico approaches: The main protease as molecular target. *EXCLI journal***2020**, *19*, 400-409.

(14) Ton, A.-T.; Gentile, F.; Hsing, M.; Ban, F.; Cherkasov, A. Rapid Identification of Potential Inhibitors of SARS-CoV-2 Main Protease by Deep Docking of 1.3 Billion Compounds. *Molecular informatics***2020**.

(15) Zhang, D.-h.; Wu, K.-l.; Zhang, X.; Deng, S.-q.; Peng, B. In silico screening of Chinese herbal medicines with the potential to directly inhibit 2019 novel coronavirus. *Journal of Integrative Medicine-Jim***2020**, *18*, 152-158.

(16) Liu, J.; Gao, J.; Li, F.; Ma, R.; Wei, Q.; Wang, A.; Wu, J.; Ruan, K. NMR characterization of weak interactions between RhoGDI2 and fragment screening hits. *Biochimica Et Biophysica Acta-General Subjects***2017**, *1861*, 3061-3070.

(17) Gao, J.; Liang, E.; Ma, R.; Li, F.; Liu, Y.; Liu, J.; Jiang, L.; Li, C.; Dai, H.; Wu, J.; Su, X.; He, W.; Ruan, K. Fluorine Pseudocontact Shifts Used for Characterizing the Protein-Ligand Interaction Mode in the Limit of NMR Intermediate Exchange. *Angewandte Chemie-International Edition***2017**, *56*, 12982-12986.

(18) Xu, D.; Li, B.; Gao, J.; Liu, Z.; Niu, X.; Nshogoza, G.; Zhang, J.; Wu, J.; Su, X.-C.; He, W.; Ma, R.; Yang, D.; Ruan, K. Ligand Proton Pseudocontact Shifts Determined from Paramagnetic Relaxation Dispersion in the Limit of NMR Intermediate Exchange. *Journal of Physical Chemistry Letters***2018**, *9*, 3361-3367.

(19) Zhang, S.; Zhong, N.; Ren, X.; Jin, C.; Xia, B. H-1, C-13 and N-15 resonance assignments of SARS-CoV main protease N-terminal domain. *Biomolecular Nmr Assignments***2011**, *5*, 143-145.

**Figure Legends**

**Figure 1.**Fragment-based screening identified three hits of SARS-CoV-2 main protease.**A**) NMR ligand-observed spectra of three hits in the presence of 10 μM full-length SARS-CoV-2 $M^{pro}$. **B**) Chemical structures of the three hits. **C**) Inhibition of enzymatic activity of SARS-CoV-2 Mpro (5 μM) by the three hits (4 mM). The negative control was carried out using the fluorescence labeled peptide (16μM) in the absence of $M^{pro}$.

**Figure 2.**Binding topology of niacin and hit 1 determined from NMR chemical shift perturbations. **A**) Superimposition of 2D $^{1}H$-$^{15}N$ HSQC spectra of SARS-CoV-2 $M^{pro}$-N in the absence and presence of niacin, respectively. Annotated are the ligand/protein molar ratios. **B**) Chemical shift perturbations induced by hit **1**. **C**) Chemical shift perturbations induced by niacin (red), hit **1** (blue) or both (green) were mapped to the surface of the crystal structure of SARS-CoV-2 $M^{pro}$ (PDB code 6LU7).

**Figure 3.**Potency and binding topology of low-molecular-weight drugs as derivatives of hit **1**. **A**) The dose-dependent inhibition of the enzymatic activity of SARS-CoV-2 $M^{pro}$ (0.5 μM) by bendamustine and emedastine, in the presence of 16 μM fluorescence labeled substrate. Error bars were estimated from three biological duplicates. **B**) The chemical shift perturbations of $^{15}N$-labeled SARS-CoV-2 $M^{pro}$-N induced by bendamustine and emedastine at the annotated ligand/protein molar ratio.

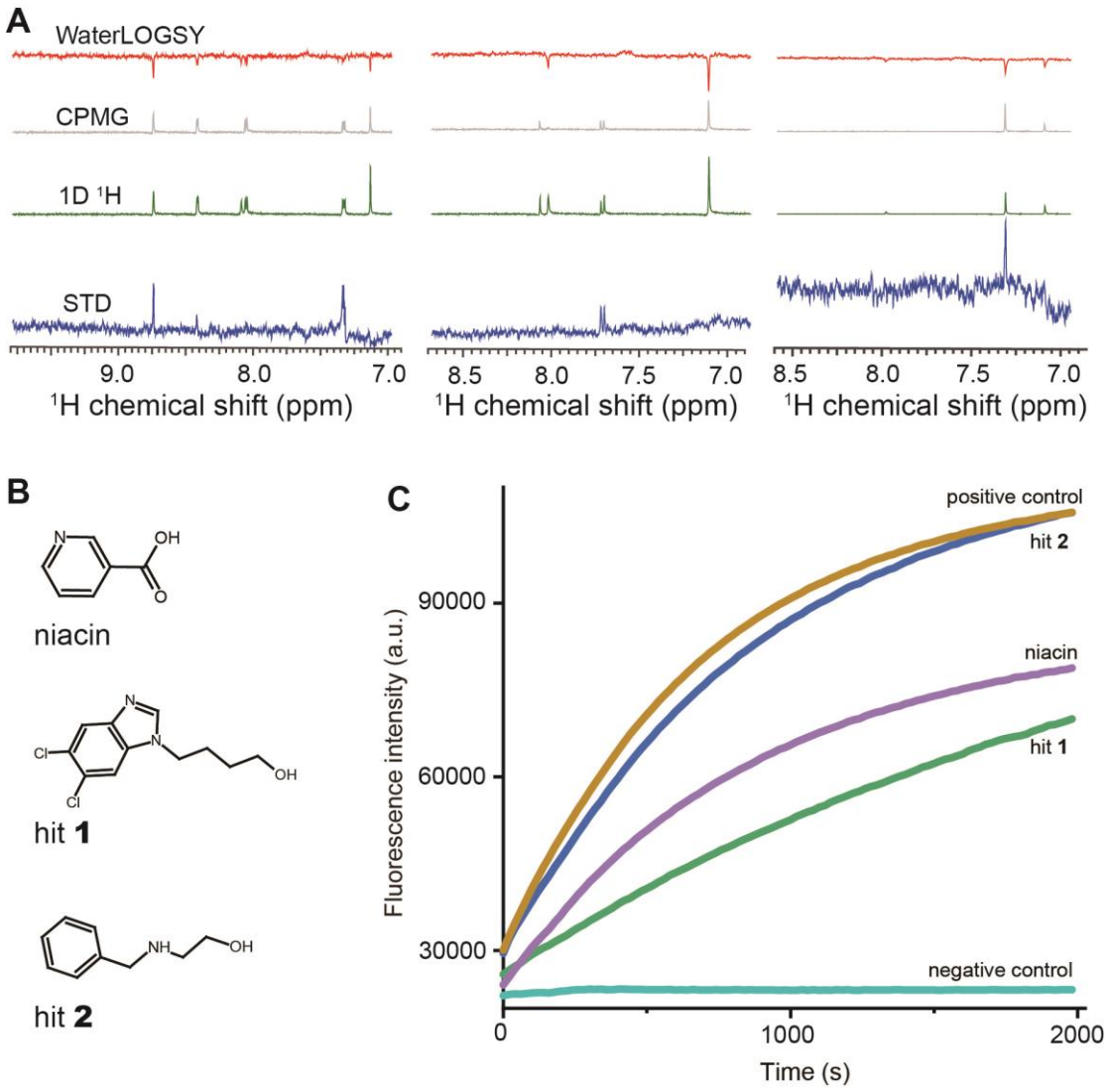
A
WaterLOGSY
CPMG
1D ¹H
STD
9.0
8.0
7.0
8.5
8.0
7.5
7.0
8.5
8.0
7.5
7.0
¹H chemical shift (ppm)
¹H chemical shift (ppm)
¹H chemical shift (ppm)
B
niacin
hit 1
hit 2
C
positive control
hit 2
niacin
hit 1
negative control
Fluorescence intensity (a.u.)
90000
60000
30000
0
1000
2000
Time (s)

**Figure1.**

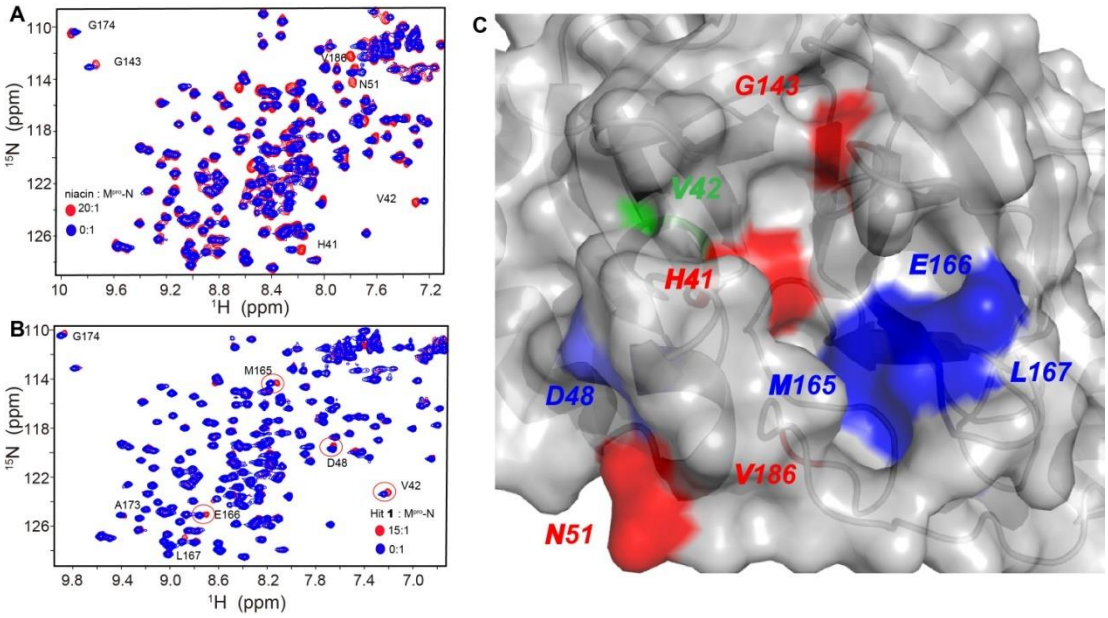
A
G174
G143
V186
N51
V42
H41
niacin : M^pro-N
20:1
0:1
15N (ppm)
1H (ppm)
B
G174
M165
D48
V42
A173
E166
L167
Hit 1 : M^pro-N
15:1
0:1
15N (ppm)
1H (ppm)
C
G143
V42
H41
E166
L167
D48
M165
V186
N51

**Figure 2.**

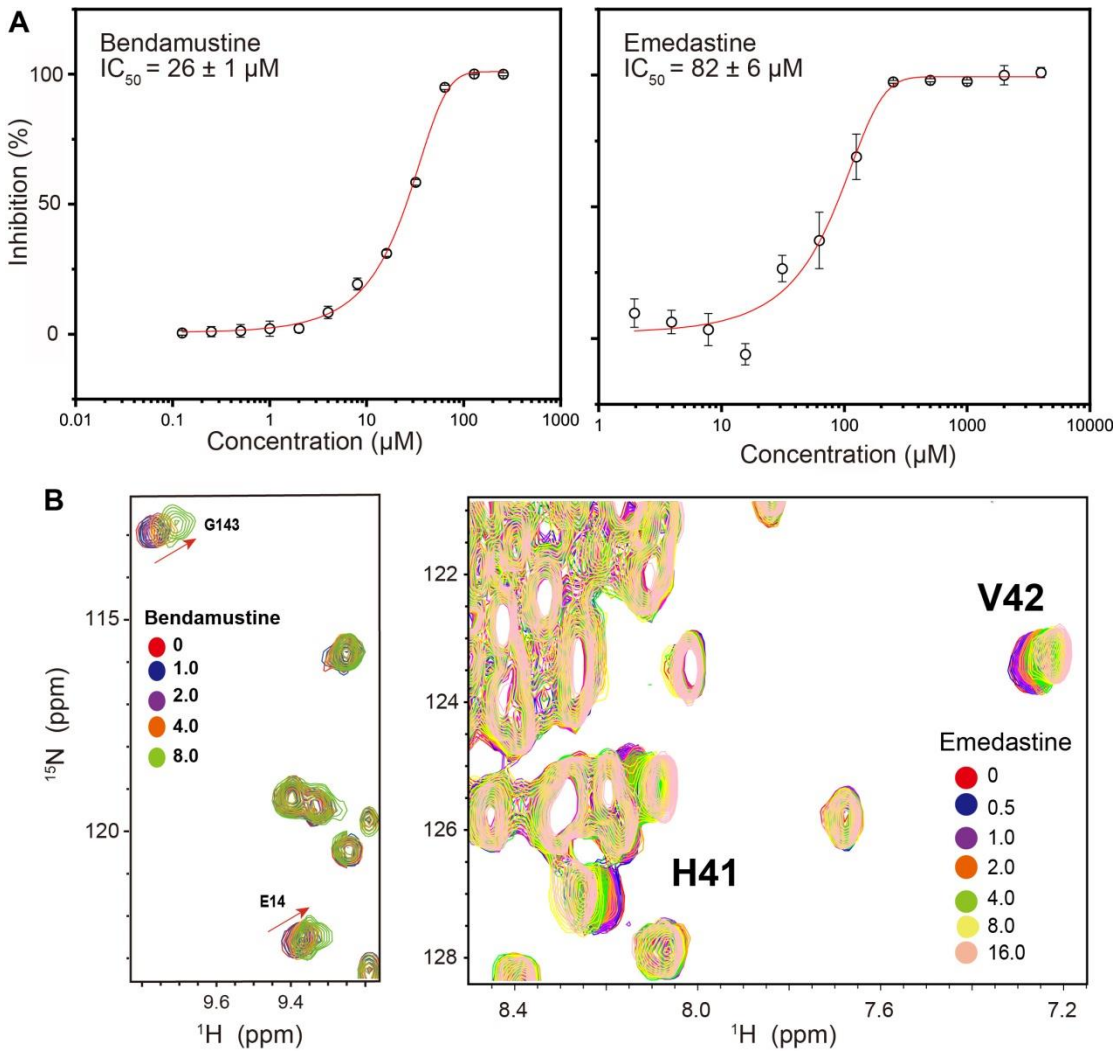
A
Bendamustine
IC50 = 26 ± 1 μM
Inhibition (%)
Concentration (μM)
Emedastine
IC50 = 82 ± 6 μM
Concentration (μM)
B
G143
Bendamustine
0
1.0
2.0
4.0
8.0
E14
15N (ppm)
1H (ppm)
V42
H41
Emedastine
0
0.5
1.0
2.0
4.0
8.0
16.0
1H (ppm)

**Figure 3.**